Mechanism of Microtubule Kinesin ATPase†

Yong-Ze Ma and Edwin W. Taylor*

Department of Molecular Genetics and Cell Biology, The University of Chicago, Cummings Life Science Center, 920 East 58 Street, Chicago, Illinois 60637

Received March 8, 1995; Revised Manuscript Received July 31, 1995[⊗]

ABSTRACT: A six-step mechanism is derived for the activation of kinesin K379 ATPase by microtubules. The data are fitted by the kinetic scheme MtK + T $\overset{1}{\rightleftharpoons}$ MtK(T) $\overset{2}{\rightleftharpoons}$ MtK·T $\overset{3}{\rightleftharpoons}$ MtK·D·P $\overset{4(-P)}{\rightleftharpoons}$ MtK·D $\overset{5}{\rightleftharpoons}$ MtK(D) $\overset{6}{\rightleftharpoons}$ MtK + D where T, D, and P refer to nucleotide triphosphate, nucleotide diphosphate, and inorganic phosphate, respectively; MtK refers to the complex of a K379 unit with the microtubule binding site. The initial binding and release steps, 1 and 6, are treated as rapid equilibria: $k_2 = 200\ s^{-1}$, $k_3 = 100\ s^{-1}$, $k_5 = 35-40\ s^{-1}$, maximum steady-state rate = $25\ s^{-1}$ (50 mM NaCl, 20 °C). k_2 was obtained from the maximum rate of fluorescence enhancement with mant-ATP as substrate, k_3 was obtained from the hydrolysis transient phase for ATP or mant-ATP, and k_5 was obtained from the rate of decrease in fluorescence of mant-ADP in the reaction K·D + Mt ⇌ MtK·D ⇌ MtK + D. A large excess of ATP was present with the Mt to block rebinding of mant-ADP. The rate was measured as a function of microtubule concentration and extrapolated to give the maximum rate k_5. The same method was used to obtain k_5 for ADP by mixing K·ADP with microtubules plus excess mant-ATP. The enhancement of fluorescence for the binding of mant-ATP is followed by a decrease in fluorescence with a rate constant of $35-40\ s^{-1}$. Since the decrease must occur after hydrolysis, it may be correlated with a step or steps leading to the low fluorescence MtK·D state. In the kinetic scheme, steps 4 and 5 both contribute to determining the maximum turnover rate. At higher ionic strengths or lower protein concentrations, the MtK complex is dissociated by ATP. The maximum rate is $12 \pm 2\ s^{-1}$ in 50 mM NaCl; consequently, hydrolysis occurs before dissociation. The dissociation constant of MtK in the presence of ADP is twice as large as the dissociation constant in the presence of ATP and four times larger than the K_M for microtubule activation. The proposed kinetic scheme, which treats the K379 units of a dimer as independent, provides a satisfactory description of the transient and steady-state properties of the system with the possible exception of results at very low substrate concentrations.

The motility properties of the microtubule kinesin system are significantly different from the actomyosin system. One kinesin molecule moves a microtubule at a velocity that is as large or larger than many kinesins acting together, and it can move more than 1 μm without detaching (Howard et al., 1989; Block et al., 1990; Romberg & Vale, 1993). The mechanism involves force generation by a transition between intermediate states of the ATP hydrolysis cycle, which produces a step motion of 8 nm (Svoboda et al., 1993). The objective of kinetic studies is to determine the set of rate and equilibrium constants of the steps in the mechanism and from this evidence to account for the velocity of motion and for the processivity that requires the order of 50 hydrolysis cycles per nucleotide site before dissociation of the motor dimer. The actomyosin cycle is nonprocessive, and myosin motors make additive contributions to the velocity (Ma & Taylor, 1994). A comparison of the kinetic mechanisms of the two types of motors may be useful in explaining the differences in properties of the two systems.

Gilbert and Johnson (1994) investigated the transient phase of ATP hydrolysis (the phosphate burst) of a microtubule−*Drosophila* kinesin construct and found a large rate constant for the hydrolysis step, greater than $100\ s^{-1}$. Their data were fitted to a four-step model in which ADP dissociation was assumed to be the rate-limiting step as was first proposed by Hackney (1988). Recently, Gilbert et al. (1995) reported a rate constant of ADP dissociation that is more than 10 times the cycle rate.

A six-step kinetic scheme was proposed previously for brain kinesin (Sadhu & Taylor, 1992), and the same mechanism with very similar rate constants was obtained for K379, a construct consisting of the first 379 amino acids of a human kinesin motor domain (Ma & Taylor, 1995). These studies are the basis for the present work in which rate constants were measured for the steps in the mechanism for the complex of K379 with microtubules, which is referred to as MtK379.[1] In solution, K379 is present mainly as a dimer (Ma & Taylor, 1995). The evidence presented here is analyzed in terms of independent K379 or MtK379 units. A possible exception in which interaction between heads effects the results is discussed in the Conclusions. Comparison of the schemes shows that binding of K379 to the microtubule increases the rate constant of the hydrolysis step 10-fold and the ADP dissociation step more than 3000-fold,

† This work was supported by Program Project Grant HL 20592 from the National Heart Lung and Blood Institute, National Institutes of Health.

⊗ Abstract published in *Advance ACS Abstracts,* September 15, 1995.

[1] Abbreviations: AMPPNP, 5′-adenylyl imidodiphosphate; EGTA, ethylene glycol bis(β-aminoethyl ether)-*N,N,N′,N′*-tetraacetic acid; mant-ATP and mant-ADP, 2′(3′)-*O*-(*N*-methylanthraniloyl)adenosine 3′-triphosphate and -diphosphate, respectively; PIPES, 1,4-piperazinediethanesulfonic acid; Mt, microtubule; K379, construct consisting of the first 379 amino acids of a human kinesin.

0006-2960/95/0434-13242$09.00/0

but ADP dissociation still makes a major contribution to limiting the rate of the cycle.

The microtubule−kinesin and actomyosin mechanisms appear to follow different pathways. Dissociation of the K379 dimer occurs after the hydrolysis step as was recently shown by Gilbert et al. (1995) while dissociation occurs before hydrolysis for actomyosin. There are significant differences in the mechanisms that could be interpreted as evidence for the coupling of a different step to force generation.

EXPERIMENTAL PROCEDURES

Preparation of Proteins and Substrates. The preparation of kinesin K379, nucleotide-free K379, and radioactive mant-ATP are described in Ma and Taylor (1995). Tubulin was prepared from porcine brain. Six to eight brains were homogenized in glutamate buffer (1 M sodium glutamate, pH 6.6, 2 mM EGTA, and 1 mM magnesium acetate) containing 0.1 mM GTP. The homogenate was clarified by centrifugation, and tubulin was partially purified from the supernatant by two cycles of polymerization and cold depolymerization in glutamate buffer plus 1 mM GTP. The tubulin was purified using a cellulose phosphate P11 column (Whatman) equilibrated with 100 mM PIPES, pH 6.9, 1 mM EGTA, 1 mM magnesium acetate, and 0.1 mM GTP and eluted with the same buffer plus 2 mM DTT. A total of 2 mM $MgCl_2$ and 1 mM GTP was added to the tubulin fractions, and the solution was frozen dropwise in liquid nitrogen and stored at −80 °C at a concentration of 5−6 mg/mL tubulin.

[^{3}H]K379 was prepared by labeling lysine groups with *N*-succinimidyl [2,3-^{3}H]propionate (Amersham) by the method described previously for myosin (Rosenfeld & Taylor, 1984). The fractional labeling is less than 1 mol/mol. The microtubule-activated ATPase and the rate constants for mant-ATP binding for a range of concentrations were not altered by labeling.

Preparation of Microtubules. Tubulin was thawed just before use. Centrifugation at 15 000 rpm for 15 min at 4 °C with or without a preincubation for 30 min on ice did not remove measurable amounts of aggregated tubulin, and this step was generally omitted. Tubulin was polymerized in 25 mM PIPES buffer, pH 6.8, 2 mM $MgCl_2$, and 15 μM taxol at 37 °C for 30 min and centrifuged through a 33% glycerol cushion at 34 °C (Ty-65 rotor, 35 000 rpm, 40 min). The pellet was resuspended in the PIPES buffer with taxol and centrifuged again through glycerol to remove free nucleotide. The pellet was resuspended in the buffer plus taxol for the experiments.

Binding of K379 to Microtubules. Binding of K379 to microtubules was determined by a sedimentation method. If necessary, the free nucleotide in the K379 solution was removed by centrifugation through a Sephadex G-25 column. [^{3}H]K379 at a concentration of 0.5 μM was centrifuged for 15 min at maximum speed (29.5 psi) in the Beckman airfuge to remove any aggregates. It was mixed with microtubules plus nucleotide at room temperature and immediately centrifuged in the airfuge at maximum speed for 15 min. Dilutions of the microtubule stock solution were made in taxol-containing buffer to maintain a taxol concentration of 10 μM. The binding was calculated from the radioactivity of an aliquot of the supernatant and an aliquot of the solution before centrifugation. The rinsed pellet dissolved in 10% SDS was also counted to obtain a second measurement of the binding and to check recovery. Variation of the time of centrifugation showed that the microtubules had essentially pelleted in 5 min.

The fractional binding in presence of ATP was measured in 5 mM MgATP. The fraction of the ATP hydrolyzed after a 5-min centrifugation at 40 μM tubulin dimer concentration in 50 mM NaCl was 0.2. Some measurements were made in 3 mM MgATP, and a set of measurements was also made using a 10 mM phosphoenol pyruvate−pyruvate kinase backup system in 50 mM KCl. The same values were obtained for binding after correction for the differences in ionic strength.

Approximately 10% of the microtubules did not pellet in 10−20 min. The microtubule concentration expressed as tubulin dimer concentration was corrected for the fraction of nonsedimenting tubulin. The same correction was made for tubulin dimer concentration in measurements of ATPase activity.

A binding measurement in AMPPNP was included in each experiment, and fractional binding was normalized to the AMPPNP value to calculate the dissociation constant. This step was included to correct for small differences in the purity of the many preparations of K379 used in these experiments.

The possibility that impurities might effect the results was investigated by centrifuging K379 with 2 mg/mL microtubules with no nucleotide added and retaining the K379 that pelleted with microtubules. The pellet was resuspended and diluted with additional microtubules for the binding and ATPase measurements. This recycled K379 sedimented quantitatively with microtubules in the presence of AMPPNP, and binding curves obtained in the presence of ATP extrapolated to a bound fraction of 0.9−1.0 at low ionic strength. The V_M of microtubule-activated ATPase was about 15% larger than for the original material. Values reported here are for recycled kinesin except for some measurements with mant-ATP as substrate. In all binding experiments, the fraction of tubulin dimer sites occupied by K379 was $\leq$0.1.

Transient Kinetics. Kinetic methods are described in Ma and Taylor (1995). The rate of dissociation of the MtK379 complex by ATP or ADP was measured in the stopped-flow apparatus by light scattering at 90° at a wavelength of 295 nm. The microtubule solution was passed through a 22 gauge needle six to eight times just before use to reduce the average length. All solutions were degassed for 30 min using an aspirator pump.

Analysis of Kinetic Data. (a) Substrate Binding and Hydrolysis Mechanism. The data are interpreted by Scheme 1. Rate or equilibrium constants are defined for each step: K_1, k_2, k_{-2}, etc. for MtK379 transitions and K'_1 and k'_2 for the K379 transitions (Ma & Taylor, 1995). Binding steps 1 and 6 are treated as rapid equilibria, and MtK(T) or MtK-(D) are relatively weakly bound complexes. The effective rate constant of substrate binding for steps 1 and 2 is $\bar{k}_2 = K_1k_2[T]/(K_1[T] + 1)$.

At high microtubule concentrations, the observed rate constants measure transitions between MtK379 states. A simplified scheme was used to analyze the transient kinetic data. The scheme is reduced to a three-step mechanism by treating the two essentially irreversible steps in the release

Scheme 1

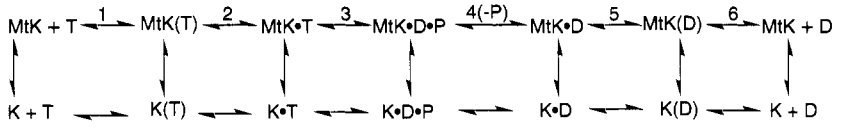

of the two products by a single effective rate constant $k_e = k_4k_5/(k_4 + k_5)$.

$$MtK \underset{k_{-2}}{\overset{\bar{k}_2}{\rightleftharpoons}} MtK{\cdot}T \overset{k_3}{\rightleftharpoons} MtK{\cdot}D{\cdot}P \overset{k_e}{\rightleftharpoons} MtK + D + P$$

and the rate equations have a simple solution for this case (Trybus & Taylor, 1982; Rosenfeld & Taylor, 1984). The time dependence of the concentration of intermediates fits two exponential terms with rate constants λ_1 and λ_2. The λ's are the roots of the quadratic equation

$$\lambda_{1,2} = 1/2[S \pm (S^2 - 4C)^{1/2}]$$

where the plus sign is taken for the larger root λ_1, S is the sum of the four rate constants, and $C = (\bar{k}_2 + k_{-2} + k_3)k_e + \bar{k}_2k_3$.

There are two limiting cases. At saturating substrate concentrations, $\bar{k}_2 = k_2$ and the two observed rate constants are approximately equal to $(k_2 + k_{-2})$ and $(k_3 + k_e)$. The value of $(k_2 + k_{-2})$ is the maximum rate constant for the enhancement of fluorescence, and $(k_3 + k_e)$ is the rate constant of the phosphate burst. In the range of very low substrate concentrations, $\bar{k}_2 \ll k_2$ or k_3 and $\bar{k}_2 = K_1k_2[T] = k^a[T]$. The two rate constants are equal to $(k^a[T] + k_e)$ and $(k_3 + k_{-2})$. Because $(k_3 + k_{-2})$ is the much larger rate constant, the coefficient of the exponential is small and the fluorescence enhancement fits a single exponential term with rate constant $(k^a[T] + k_e)$.

The experiments measure total phosphate at time t:

$$P(t) = MtK{\cdot}D{\cdot}P + k_e\int(MtK{\cdot}D{\cdot}P)dt$$

The size of the phosphate burst per site (B) defined as the intercept of the linear phase on the zero time axis is obtained from the intergral:

$$B = V[1/k_e - (\lambda_1 + \lambda_2)/(\lambda_1\lambda_2)]$$

where V is the steady-state rate per site. If λ_1 is much larger than λ_2, the equation reduces to

$$B = V(1/k_e - 1/\lambda_2)$$

which is the result given in Rosenfeld and Taylor (1984), which can be consulted for the derivation.

(b) Dissociation of mant-ADP or ADP from the MtK·D Complex. This step was measured for mant-ADP by mixing the complex of K379 and mant-ADP with microtubules plus excess ATP to block rebinding of mant-ADP:

$$K{\cdot}D^* + MT \rightleftharpoons MTK{\cdot}D^* \xrightarrow{k_5} MtK + D$$

where the asterisk indicates fluorescence enhancement of the bound nucleotide. The microtubule site concentration, expressed as tubulin dimer concentration, is in large excess over the K379 concentration. The fluorescence transient fitted a single exponential term, and the rate constant fitted a hyperbolic dependence on microtubule concentration. k_5 was obtained by extrapolation of the hyperbolic dependence. The tubulin dimer concentration for half-maximum rate defines an apparent dissociation constant for the K·D* complex.

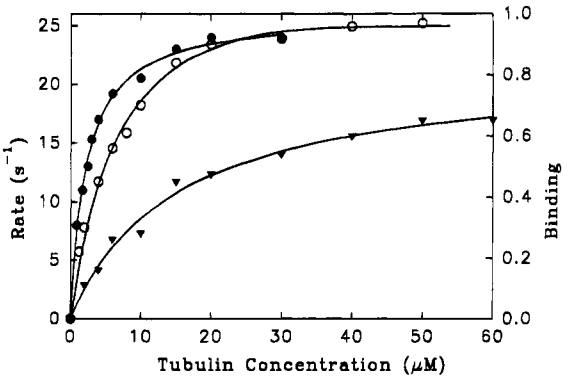

FIGURE 1: MtK379 ATPase activation and binding of K379 to microtubules in presence of ATP and ADP. ATPase activity (●) is expressed per K379 monomer unit; fractional binding of [^{3}H]-K379 in the presence of ATP (○) and ADP (▼) measured by sedimentation assay. Microtubule concentration is expressed as tubulin dimer concentration. The smooth curves are hyperbolas fitted to data points. Conditions: 0.5 μM K379 or [^{3}H]K379, fractional occupancy of tubulin dimer sites ≤0.1, 25 mM NaCl, 25 mM PIPES, pH 6.9, 7 mM $MgCl_2$, 5 mM ATP or 5 mM ADP, and 1 mM EGTA, at 22 °C.

The corresponding reaction for dissociation of ADP was measured by reacting the complex of K379 and ADP with microtubules plus mant-ATP. The ratio of mant-ATP concentration to bound ADP was chosen such that the rate of binding of mant-ATP to a free MtK379 site was four to five times larger than the rates observed in the experiments so that the rate of ADP dissociation limits the rate of mant-ATP binding. The rebinding of ADP cannot be neglected, and the value obtained for rate constant k_5 is estimated to be 10% too large based on simulation of the rate equations.

RESULTS

Activation of K379 ATPase by Microtubules. The ATPase activity of K379 of 0.01 s^{-1} at 20 °C is increased about 2500-fold by microtubules. The dependence of the rate of hydrolysis on microtubule concentration is shown in Figure 1. The maximum rate per site (V_M) obtained by a fit to a hyperbola is 26 s^{-1}, and it is independent of ionic strength up to 100 mM in NaCl. K_M(Mt), the tubulin dimer concentration at half-maximum rate, is 2 μM in Figure 1 (25 mM NaCl plus 5 mM Mg ATP), but it increased markedly with ionic strength (Table 1). At 150 mM NaCl, the variation in rate with concentration is nearly linear in the accessible range of microtubule concentrations and the maximum rate could not be obtained by extrapolation, but the value is larger than 15 s^{-1}.

The V_M for mant-ATP is the same as for ATP within 10%. A value of 20 s^{-1} for a range of ionic strengths was obtained versus 22−24 s^{-1} for ATP on the same preparation of K379

Table 1: Steady-State Rate Constants and Dissociation Constants of MtK379[a]

NaCl (mM)	V_M (s^{-1})	K_M(Mt) (μM)	K^d MtK379 [ATP] (μM)	max binding	K^d MtK379 [ADP] (μM)	max binding
25	26 ± 1	1.1 ± 0.3	4.2 ± 0.1	0.96 ± 0.01	5.3	0.96
50	27 ± 1	2.7 ± 0.3	8.3 ± 1	0.9 ± 0.1	17 ± 1	0.83 ± 0.02
75	26 ± 1	5.4 ± 1.4	20 ± 3	0.7 ± 0.1	25 ± 2	0.75 ± 0.01
100	27 ± 1	11 ± 2	25 ± 6	0.6 ± 0.1		

[a] Dissociation constants are expressed as tubulin dimer concentration. K_M(Mt), tubulin dimer concentration for half-maximum ATPase activation; V_M, extrapolated maximum ATPase rate per K379 (s^{-1}); K^d MtK379 [ATP], dissociation constant of MtK379 in the presence of ATP; K^d MtK379 [ADP], dissociation constant of MtK379 in the presence of ADP; Data given as mean ± standard deviation of three or four experiments. Conditions: 25 mM PIPES, pH 6.9, 2 mM $MgCl_2$, 1 mM EGTA (the standard buffer), plus NaCl as indicated, at 22 °C. ATPase measured in 1 mM MgATP (1 mM ATP plus 1 mM $MgCl_2$); binding in presence of ATP measured in 5 mM MgATP; binding in presence of ADP measured in 3 mM MgADP.

Table 2: Steady-State Constants for mant-ATP as Substrate and Rate of mant-ADP Dissociation[a]

NaCl (mM)	V_M (s^{-1})	K_M(Mt) (μM)	max rate mant-ADP dissoc (s^{-1})	Mt concn at half-max rate (μM)
25	20	3	38 ± 2	5 ± 0.5
50	22	7 ± 2	39 ± 1	13 ± 1
75	20	17 ± 3	27 ± 3	20 ± 4
100	16 ± 1	24 ± 1		

NaCl (mM)	K^d MtK379 [mant-ATP] (μM)	K^d MtK379 [mant-ADP] (μM)
50	12 ± 2	18 ± 3

[a] Conditions as in Table 1. K379 preparations not recycled for mant-ATPase measurements. V_M for ATP on the same preparation was 22–24 s^{-1} for NaCl concentrations of 25, 50, and 75 mM. K^d MtK379 [mant-ATP] or [mant-ADP] is the dissociation constant of MtK379 in the presence of 3 mM mant-ATP or 3 mM mant-ADP, respectively. Maximum rate of dissociation of mant-ADP measured by displacement by microtubules in the presence of 0.5 mM ATP (see Figures 6 and 7). Microtubule concentration for half-maximum rate defines an apparent dissociation constant of the K379–mant-ADP complex. The value is 16 μM in 50 mM NaCl for displacement in presence of 3 mM ATP for comparison with dissociation constants of MtK379.

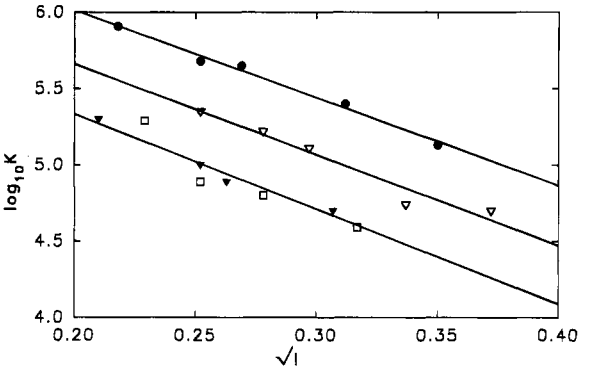

FIGURE 2: Dependence of apparent binding constants on ionic strength. The logarithm (base 10) of the apparent binding constants (the reciprocals of the dissociation constants) are plotted against the square root of ionic strength; (●) concentration of microtubule for half-maximum activation of ATPase (K_M(Mt)); (▽) apparent binding constant of K379 to microtubules in the presence of ATP; (□) binding constant of K379 to microtubules in the presence of ADP; (▼) apparent binding constant of K379–mant-ADP complex determined by the kinetic method described in Figure 7. Values are given in Tables 1 and 2. The ionic strength $I = (1/2)\Sigma(Z_i)^2C_i$ where Z_i is the charge on ion species of molar concentration C_i. The contributions of PIPES buffer, $MgCl_2$, and Mg nucleotides are included in the sum.

(not recycled). However the K_M(Mt) was twice as large as for ATP (Table 2).

The dependence of the ATPase on ATP concentration at 25 μM microtubule concentration fitted a hyperbola with K_M(ATP) of 40 μM in 50 mM NaCl. In 100 mM salt, the value was approximately 80 μM (data not shown). The K_M(mant-ATP) was 30–40 μM in 50 mM NaCl.

Effects of Nucleotides on the Binding of K379 to Microtubules. In the absence of nucleotides, the dissociation constant of the MtK379 complex is very small, but it is dramatically increased in the presence of ATP or ADP. The binding of K379 to microtubules was determined by a sedimentation method, and binding curves in the presence of 5 mM MgATP and 5 mM MgADP are shown in Figure 1. Half-maximum binding occurs at a tubulin dimer concentration of 4 μM in presence of ATP compared to 2 μM for half-maximum activation at the same ionic strength and ATP concentration. In presence of ADP, half-maximum binding requires a tubulin dimer concentration of 12–13 μM. Binding curves gave a good fit to a hyperbola, and the apparent dissociation constants for a range of ionic strengths are given in Table I.

Binding measurements were made in 5 mM Mg ATP while 1 mM Mg ATP was used for most ATPase measurements, and the nucleotide makes a large contribution to the ionic strength. In order to compare apparent dissociation constants, the data are plotted in Figure 2 against the square root of total ionic strength. The plots have essentially the same slope; consequently, all of the data can be used to calculate the ratio of apparent dissociation constants from the spacing between the curves. The dissociation constant of MtK379 in presence of ADP is 2.2 times larger than the average dissociation constant in presence of ATP, which in turn is 2.3 times larger than the K_M(Mt) for microtubule activation.

At low ionic strength, the binding curves in the presence of ADP or ATP extrapolated to 0.85–1.0 for several preparations. At higher ionic strengths, although the extrapolation is subject to larger errors, the maximum binding showed a trend to lower values (Table 1). A possible explanation is partial dissociation of a K379 dimer since measurements of the value of the molecular weight by sedimentation equilibrium were smaller than the value for a dimer in 150 mM NaCl (Ma & Taylor, 1995). In experiments to be described elsewhere, it was found that monomeric constructs have larger values for the dissociation constants.

The plots against ionic strength (Figure 2) are linear up to 100 mM in NaCl concentration. The slope is proportional to the product of the number of charges in the binding site, and since it does not depend on nucleotide, the same slope is expected for the MtK379 complex. The dissociation constant is approximately 0.3 μM in 100 mM NaCl, although

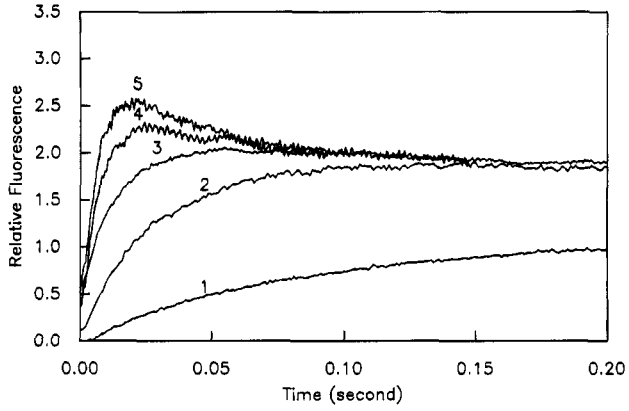

FIGURE 3: Fluorescence enhancement for the binding of mant-ATP to the MtK379 complex. A series of fluorescence transients were recorded on the same time scale and superimposed to illustrate the change in shape of the transient signal. The numbers 1−5 refer to mant-ATP concentrations after mixing of 3, 10, 25, 50, and 75, μM respectively. The signals were approximately normalized to show the change in amplitude of fluorescence enhancement per K379 site. The final level of the fractional increase in fluorescence is constant for concentrations $\geq$50 μM. Data collection begins 3−4 ms before flow stops, which is observed as the initial delay in the increase of fluorescence for trace 2. Conditions: 15 μM microtubules, 1−12.5 μM K379, 150 mM NaCl, 25 mM PIPES, pH 6.9, 2 mM $MgCl_2$, and 1 mM EGTA, at 20 °C.

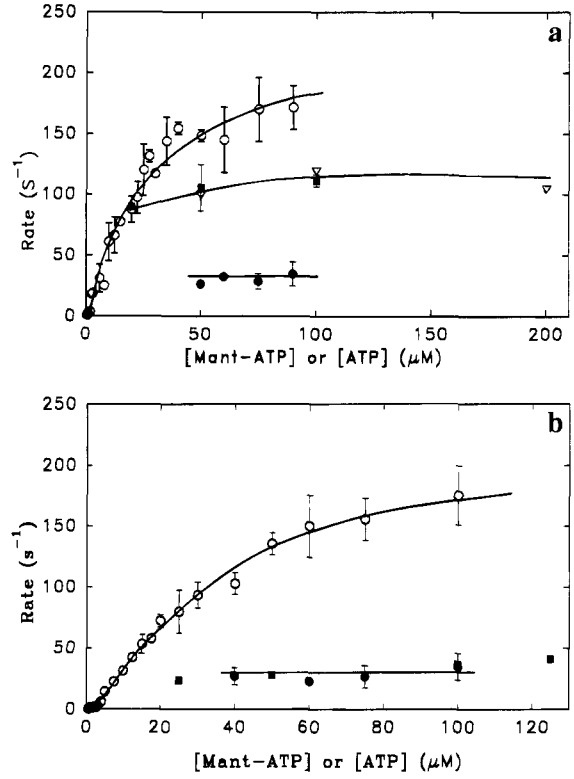

FIGURE 4: Dependence on substrate concentration of the two apparent rate constants for the binding of mant-ATP and the rates of the hydrolysis step for ATP and mant-ATP. (a) NaCl concentration 50 mM. The rate constants were obtained by fitting the fluorescence transient to one exponential term at low substrate concentrations and to two exponential terms at higher concentrations. Apparent rate constant for the increase (○) in fluorescence was fitted to a hyperbola for mant-ATP concentrations greater than 5 μM; the decrease in fluorescence (●) was fitted to a straight line; 12.5 μM microtubules, K379 concentration was varied from 0.2 to 12.5 μM to keep the ratio of mant-ATP to K379 at least 4:1. Error bars are standard deviation for three to five traces; bars are omitted if the range is smaller than the symbol. Transient rate constant of phosphate burst with ATP (■) or mant-ATP (▽) as substrate. The smooth curve was drawn through the data points. (b) NaCl concentration 150 mM. Apparent rate constants for increase (○) and decrease (●) of fluorescence enhancement and rate constant of phosphate burst with ATP as substrate (■). Other conditions: 25 mM PIPes, pH 6.9, 2 mM $MgCl_2$, and 1 mM EGTA, at 20 °C.

the value may be overestimated if the nucleotide has not been completely removed. In 50 mM NaCl, the calculated value is 50−60 nM. Based on these values, the binding constant of K379 to the microtubule is reduced by roughly 100-fold in the presence of ATP and more than 200-fold by the binding of ADP.

The dissociation constant of MtK379 in presence of mant-ATP is about twice as large as for ATP (Table 2). A binding curve in the presence of mant-ATP in 50 mM NaCl is included in Figure 9.

Substrate Binding Steps of the Microtubule−K379 Complex. The binding of mant-ATP to brain kinesin and K379 gave a two-step fluorescence change, an increase followed by a decrease (Sadhu & Taylor, 1992; Ma & Taylor, 1995). The binding of mant-ATP to the MtK379 complex, which was formed from nucleotide-free K379, gave a fluorescence signal that is very similar to nucleotide-free K379. A series of fluorescence transients on the same time scale are shown superimposed in Figure 3. At low concentrations of mant-ATP, the fluorescence increased to a maximum value, and the time course gave an approximate fit to one exponential term. As the concentration was increased, the fluorescence signal passed through a maximum and then decreased. The curves in Figure 3 are approximately normalized to the initial fluorescence to illustrate the change in amplitude with concentration. In the higher concentration range, the enhancement decreases to the same final value.

The rate constants for representative experiments are plotted in Figure 4 for a microtubule concentration of 12.5 μM and NaCl concentrations of 50 and 150 mM. The two ionic strengths were chosen to give conditions leading to high association versus nearly complete dissociation of MtK379 in the steady state. The observed rate constant for the increase in fluorescence approached 200 s^{-1}, which is similar to the value obtained for kinesin or K379. The maximum rate, obtained by fitting the concentration dependence to a hyperbola for substrate concentrations greater than 5 μM, is approximately 250 s^{-1} in 50 and 150 mM NaCl (Table 3), but the errors in extrapolation are large. In terms of the three-step kinetic scheme, the maximum rate is approximately equal to $(k_2 + k_{-2})$.

In the low concentration range (0.5−3 μM), the rate constant increased linearly with substrate concentration, but the curve deviated from the hyperbola. The deviation is seen more clearly at high ionic strength (Figure 4b). Plots on an expanded scale gave an initial linear region with slope of 0.85×10^6 M^{-1} s^{-1} in 150 mM NaCl and 1.7×10^6 M^{-1} s^{-1} in 50 mM NaCl. The slope is 3 times smaller than the initial slope of a hyperbola. The intercept at zero concentration is less than 1 s^{-1} for both ionic strengths.

The rate constant of the decrease in fluorescence of MtK379 is essentially constant over the higher range of substrate concentrations. The value is 30−40 s^{-1} compared to 10 s^{-1} for K379 and brain kinesin. Rate constants for the phosphate burst phase are also included in Figure 4 for comparison with the rate constants measured by fluorescence.

Table 3: Rate Constants of Nucleotide Binding Reactions of MtK379[a]

substrate	ionic strength (mM NaCl)	k^a (M^{-1} s^{-1})	max rate	rate of fluorescence decrease (s^{-1})
mant-ATP	50	1.7×10^6	250 ± 30	40 ± 3
	150	0.85×10^6	250 ± 40	30 ± 3
mant-ADP	50	1.1×10^6	350 ± 40	
	150		300 ± 50	40 ± 5

[a] Rate constants for fluorescence enhancement for mant-ATP and mant-ADP versus substrate concentration were fitted to a hyberbola for concentrations greater than 5 μM to obtain the maximum rate. Error limits refer to estimated error of fitted parameter. k^a is the initial slope for the very low substrate concentrations (<2 μM). Rate of fluorescence decrease phase is essentially independent of concentration; values refers to average and standard deviation over the concentration range. Decrease phase was not present for mant-ADP in 50 mM NaCl. Conditions: 25 mM PIPES, pH 6.9, 2 mM $MgCl_2$, and 1 mM EGTA at 20 °C.

The amplitude of the decrease in fluorescence increased by a factor of 2 with an increase in ionic strength from 25 to 150 mM NaCl at a fixed protein and substrate concentration (10 μM K379, 12.5 μM tubulin dimer, and 90 μM mant-ATP) while the rate constant decreased by 30% over this range.

The binding of mant-ADP to microtubule K379 at high ionic strength (150 mM NaCl) gave rate constants very similar to mant-ATP, an increase with maximum rate of more than 200 s^{-1} followed by a decrease at 40 s^{-1}. At low ionic strength for which the system is largely associated, the decrease in fluorescence was not observed. Values of the rate constants are summarized in Table 3.

Phosphate Burst Phase and the Rate of the Hydrolysis Step. The transient phase of ATP hydrolysis is significantly different for the MtK379 complex compared to K379 alone. Representative experiments for the transient phase of ATP and mant-ATP hydrolysis are shown in Figure 5. In 150 mM NaCl, the rate constant of the transient phase is 35 s^{-1} at 100 μM ATP, and the steady-state rate is 2 s^{-1} (Figure 5a). The size of the initial burst, the intercept of the linear phase on the zero time axis, is approximately 0.6 expressed relative to the molar concentration of K379. The experiments were done with nucleotide-free protein in order to compare rate constants in the presence and absence of microtubules using K379 that had received the same treatment. The size of the burst is not corrected for a decrease in available nucleotide binding sites in preparing nucleotide-free protein. The burst size for MtK379 is actually larger than for K379, possibly because the protein is more stable in the complex with microtubules and less prone to loss of binding sites by aggregation.

The rate constant of the transient phase increased with ATP concentration in the range from 30 to 125 μM (data included in Figure 4). The maximum rate is approximately 45−50 s^{-1}. The complex is more than 90% dissociated when the steady state is reached, yet the rate constant of the hydrolysis step is 5 times larger than for K379.

In 50 mM NaCl and 25 μM microtubule sites, the rate of the transient exceeds 100 s^{-1} at an ATP concentration of 100 μM, and the size of the burst was reduced to 0.3−0.4 (Figure 5b). The transient rate for mant-ATP is essentially the same as for ATP, and both substrates gave a steady-state rate of 10−12 s^{-1} in this experiment. The rate of the

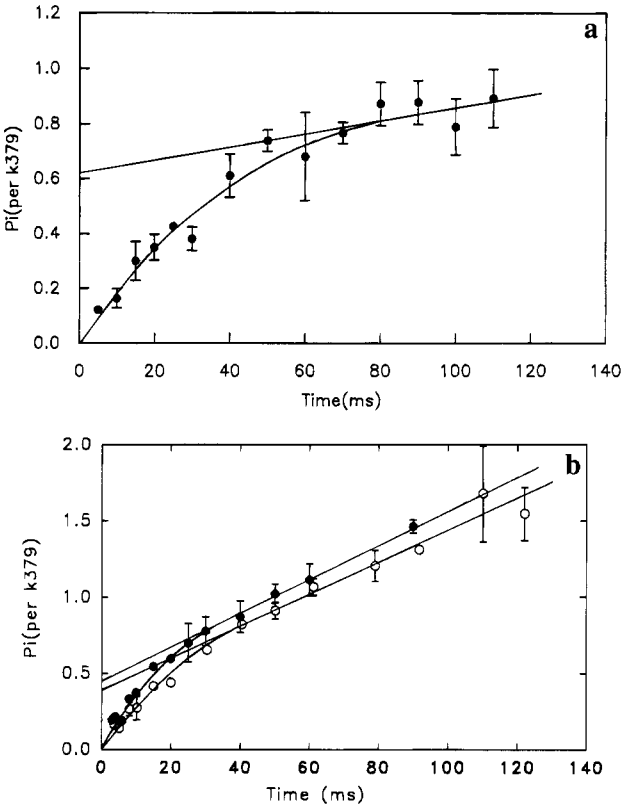

FIGURE 5: Phosphate burst phase of MtK379. Measurements were made in a quench flow apparatus up to 120 ms; steady-state rate was also measured by hand mixing on a longer time scale. (a) NaCl concentration 150 mM. Phosphate formation is expressed per nucleotide-free K379 monomer unit. No correction was made for possible loss of nucleotide binding sites. Smooth curve is the fit to one exponential plus a linear term by simplex method (PSI plot program). The steady-state rate is 2 s^{-1}; the transient rate constant is 35 s^{-1}; error bars are the range of duplicate measurements. Conditions: 13 μM K379, 14 μM microtubules, and 100 μM [γ-^{32}P]ATP. (b) NaCl concentration, 50 mM; (●) ATP; (○) mant-ATP. The steady state rate is 10−12 s^{-1} for both substrates, and the rate of the transient phase is approximately 100 s^{-1}. For ATP experiments: 20 μM microtubules, 12.5 μM K379, and 100 μM [γ-^{32}P]ATP. For mant-ATP experiments: 22.5 μM microtubules, 20 μM K379, and 280 μM [γ-^{32}P]mant-ATP. Conditions: 25 mM PIPES, pH 6.9, 2 mM $MgCl_2$, and 1 mM EGTA, at 20 °C.

transient increased slightly with substrate concentration in the range from 50 to 200 μM (data included in Figure 4). The maximum rate is at least 120 s^{-1}, but the rate constant is too large and the burst is too small to measure the rate constant accurately by extrapolation versus substrate concentration.

A burst size much smaller than unity does not mean that a large fraction of the nucleotide-free K379 has been inactivated or does not give a phosphate burst when complexed with microtubules. The burst size in 50 mM NaCl of a MtK379 complex that was treated with apyrase to remove ADP and assayed immediately was still 0.4 while the value for K379 was 0.9. In terms of the three-step model, the burst size can be calculated from the rate constants λ_1 for the fluorescence transient, λ_2 for the hydrolysis transient, V for the steady-state rate in the experiment, and a value for k_e assumed to be 20 s^{-1} for the experiments in 50 mM NaCl. The calculated value is 0.4−0.5, which is slightly larger than the values obtained. Therefore, the small size of the burst is a consequence of the large rate of completion of the cycle. The results indicate that at least 80% of the K379 contribut-

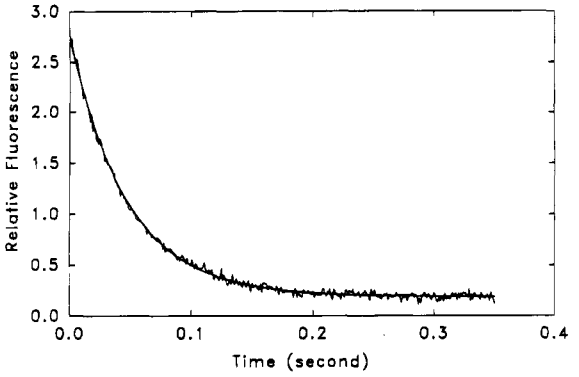

FIGURE 6: Dissociation of mant-ADP from the MtK379 mant-ADP complex. The jagged curve is the fluorescence signal for the dissociation of mant-ADP, and the smooth curve is the fit to one exponential term with a rate constant of 21 s^{-1}. 10μM microtubule plus 250 μM ATP were mixed with 1 μM K379 mant-ADP complex (concentration after mixing 1:1). Conditions: 25 mM PIPES, pH 6.9, 50 mM NaCl, 2 mM $MgCl_2$, and 1 mM EGTA, at 20 °C.

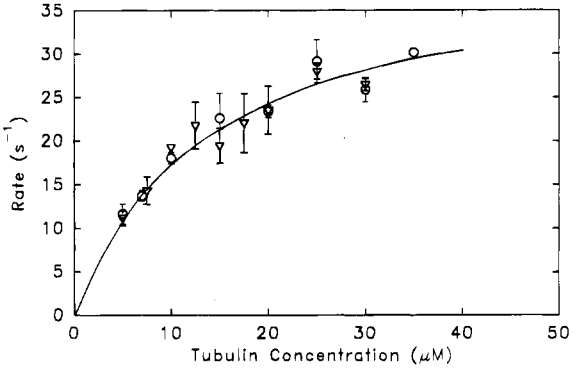

FIGURE 7: Rate constants for dissociation of mant-ADP and ADP from MtK379 nucleotide complex. Rate constant for dissociation of mant-ADP (O) was obtained from reaction of K379−mant-ADP with microtubules plus ATP as described in Figure 6. Rate constant for dissociation of ADP (▽) was obtained from the rate constant for increase in fluorescence for the reaction of the K379−ADP complex with microtubules plus mant-ATP. For details, see text. The smooth curve is the fit of both data sets to a hyperbola. The extrapolated maximum rate of 40 s^{-1} is the rate constant of dissociation of ADP or mant-ADP from MtK379 nucleotide diphosphate complex. The concentration at half maximum rate is 13 μM (tubulin dimer concentration), which defines an apparent dissociation constant for the K379 nucleotide diphosphate complex. Conditions: 25 mM PIPES, pH 6.9, 50 mM NaCl, 2 mM $MgCl_2$, 1 mM EGTA, and 1 μM K379 mant-ADP complex mixed with 0.5 mM ATP plus microtubules or 2−7.2 μM K379 ADP complex mixed with 10−25 μM mant-ATP plus microtubules.

ing to the transient and that in terms of a dimer, both heads hydrolyze ATP.

ADP Dissociation Step. The rate of mant-ADP dissociation was measured by mixing the K379 mant-ADP complex with microtubules plus excess ATP to block rebinding of the mant-ADP. The decrease in fluorescence is illustrated in Figure 6. The signal fits a single exponential term with no evident lag phase. Measurements of the rate constant as a function of microtubule concentration are plotted in Figure 7. The points fit a hyperbolic dependence, and the maximum rate obtained by extrapolation is 38 s^{-1}. The maximum rate is the rate constant of mant-ADP dissociation from the MtK·D complex. The tubulin dimer concentration at half-maximum rate defines an apparent dissociation constant for the complex of K379 with mant-ADP (see Analysis of Kinetic Data). The turnover rate of MtK379 for mant-ATP

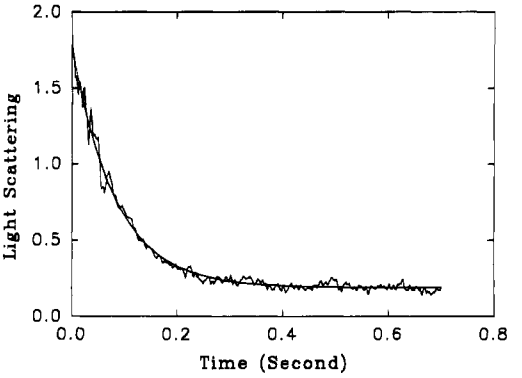

FIGURE 8: Dissociation of MtK379 complex by ATP. MtK379 complex, 1.25 μM (1 mol of K379/mol of tubulin dimer) was reacted with 750 μM ATP (concentrations after mixing). The jagged curve is the light-scattering signal at 295 nm, and the smooth curve is the fit to one exponential term with a rate constant of 12 s^{-1}. Conditions: 25 mM PIPES, pH 6.9, 50 mM NaCl, 2 mM $MgCl_2$, and 1 mM EGTA, at 20 °C.

was 20 s^{-1} for the same preparation. Values for the rate constant (k_5) and the apparent dissociation constant for several experiments are given in Table 2 for a range of ionic strengths.

The rate constant of ADP dissociation was measured by the same method. The complex of K379 with ADP was mixed with microtubules plus mant-ATP at a ratio of at least 5 mant-ATP:1 bound ADP. The rate constant of increase of fluorescence measures the rate at which ADP is released from the site. Values are also plotted in Figure 7. The extrapolated maximum rate is 35 s^{-1}, and half-maximum rate is attained at 13 μM tubulin dimer concentration. The maximum rates for ADP and mant-ADP are not different within the error of the extrapolation, and data for both nucleotides are fitted to a single curve in Figure 7.

Rate of Dissociation of the MtK379 Complex. At high ionic strength or low protein concentrations, the MtK379 complex is dissociated by ATP or ADP. The rate of dissociation of MtK379 was measured by the decrease in 90° light scattering. The scattering of a microtubule solution relative to buffer increased approximately 1.6−1.8-fold by addition of one K379 monomer unit per tubulin dimer (one K379 dimer per two tubulin dimers). Although a larger light-scattering change is obtained at a ratio of one K379 dimer per tubulin dimer, the experiments were done at the lower ratio to avoid possible complications from saturation of the microtubule lattice (Hackney, 1994a).

A problem with the use of light scattering to measure dissociation is that mixing microtubules or the MtK379 complex with buffer in the stopped-flow apparatus caused a small decrease in light scattering. The effect was reduced by shearing the microtubules before use, but the size of the artifact was 20−25% of the decrease in scattering for dissociation of the complex. Fitting of the artifact to an exponential gave a rate constant of 5−6 s^{-1}.

The decrease in light scattering for the reaction of 1.25 μM MtK379 with 0.75 mM ATP (concentrations after mixing) in 50 mM NaCl is shown in Figure 8. The transient gave a good fit to a single exponential with a rate constant of 12 s^{-1} and no evident lag phase. If it is assumed that the artifact is present but not resolved from the signal, the fitted rate constant could be 15% smaller than the actual value. At the protein concentration used in the experiments, the

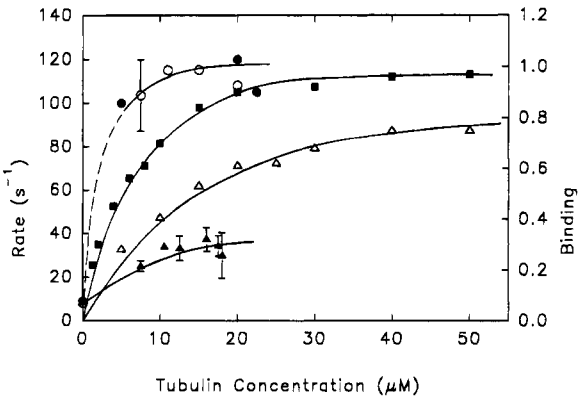

FIGURE 9: Dependence on microtubule concentration of the rate of the phosphate burst and the rate of decrease in fluorescence. The rate constants for the phosphate burst for ATP (○) and mant-ATP (●) and the rate constants for decrease in fluorescence (▲) are plotted against microtubule concentration. The fractional binding of K379 to microtubules in the steady state is shown for ATP (■) and mant-ATP (△) at approximately the same ionic strength. Points at zero microtubule concentration are for K379. Conditions: phosphate burst measured at 100 μM [γ-^{32}P]ATP and 200 μM [γ-^{32}P]mant-ATP except for the first point for each nucleotide, which is 50 μM. Binding of K379 to microtubules was measured by sedimentation assay, with the addition of 3 mM $MgCl_2$ and 3 mM mant-ATP or 5 mM $MgCl_2$ and 5 mM ATP to standard buffer. NaCl concentration is 50 mM except for the ATP binding experiments, which were done in 25 mM NaCl to compensate for the contribution of the Mg ATP to the ionic strength. Other conditions: standard buffer, 25 mM PIPES, pH 6.9, 2 mM $MgCl_2$, and 1 mM EGTA, at 22 °C.

complex should be nearly completely dissociated based on steady-state binding measurements (Table 1).

The rate constant increased with ATP concentration to a maximum of 12 ± 1 s^{-1} in 50 mM NaCl and 16 ± 2 s^{-1} in 150 mM NaCl. The concentration of ATP for half-maximum rate could not be determined accurately because the rate decreased to 5−6 s^{-1} at 25−50 μM ATP, and at lower ATP concentrations the dissociation step was not separable from the artifact. A complex of nucleotide-free kinesin with microtubules gave a similar value for the maximum rate of dissociation by ATP.

It was shown by the sedimentation assay that ADP dissociates MtK379 more effectively than ATP. Light-scattering measurements gave a maximum rate of dissociation of 12 ± 2 s^{-1} by ADP for both ionic strengths.

Effect of Microtubule Concentration on Rate Constants of Phosphate Burst and Fluorescence Decrease. The rate of dissociation of MtK379 by ATP is almost 10 times smaller than the rate of the hydrolysis step, which indicates that hydrolysis occurs before dissociation. Further evidence for this conclusion was obtained by measuring the rate constants for the phosphate burst and the decrease in fluorescence for a range of microtubule concentrations such that MtK379 is largely dissociated to nearly completely associated in the steady state. Rate constants are plotted in Figure 9 together with measurements of the fractional steady state association for ATP and mant-ATP as substrates.

The results are most striking for mant-ATP as substrate. There is a large increase in the degree of dissociation of MtK379 for very little decrease in the rate of the phosphate burst or the rate of the decrease in fluorescence. At the lowest MtK379 concentration, it was necessary to reduce the substrate concentration to 50 μM to obtain sufficient fractional hydrolysis of the substrate, and the lower rate constant is mainly caused by the dependence of the burst rate on substrate concentration.

Therefore, under conditions such that the MtK379 complex is largely dissociated by the end of the transient phase, the rate constants of the hydrolysis and fluorescence decrease steps are hardly effected and are several times larger than the values of 10 s^{-1} for the hydrolysis and fluorescence decrease steps for K379 in the absence of microtubules.

CONCLUSIONS

The steps in binding of substrate, the hydrolysis step and the dissociation of ADP, were measured for the MtK379 complex. The corresponding steps for K379 are reported in Ma and Taylor (1995). The minimum kinetic scheme for both reactions is shown in Scheme 1 where T, D, and P refer to nucleotide triphosphate, nucleotide diphosphate, and inorganic phosphate, respectively. Equilibrium or rate constants K_1, k_2, etc. are defined for the numbered steps for MtK379, and K'_1, k'_2 etc. are defined for the K379 steps. The fluorescent substrate analogs were used to measure the steps in nucleotide binding, and the rate of the isomerization at step 2 is known only for mant-ATP. However, a complete set of measurements of the steps was made with mant-ATP and mant-ADP, and the rate constants agreed with the values for ATP and ADP within 20%. The main difference is that the dissociation constants of MtK379 in the presence of mant-ATP and mant-ADP are about 1.5−2 times larger than for ATP and ADP, respectively.

Effects of Microtubule Binding on K379 ATPase. The maximum rate of fluorescence enhancement for the binding of mant-ATP and the concentration for half-maximum rate are similar for MtK379 and K379. The maximum rate is approximately equal to ($k_2 + k_{-2}$), and the increase of 30−50 s^{-1} for MtK379 compared to K379 could be an increase in the contribution from k_{-2}. Also, the initial slope of rate versus concentration gives k^a equal to 1.7 × 10^6 M^{-1} s^{-1} in 50 mM NaCl. The value of V_M/K_M(ATP) has the dimensions of a second-order rate constant, and it is approximately 10^6 M^{-1} s^{-1}. For the kinetic scheme in which the steps after step 2 are irreversible, it is easily shown that V_M/K_M(ATP) is equal to $k^a/(1 + k_{-2}/k_3)$. The two values are in reasonable agreement if k_{-2}/k_3 is 0.5, which gives 50 s^{-1} for k_{-2}. Therefore, the initial substrate binding and isomerization steps are not affected by interaction with the microtubule except for a possible reduction in the binding constant of ATP from an increase in k_{-2}.

The rate constant of the hydrolysis transient is increased from 9 ± 1 s^{-1} for nucleotide-free K379 to at least 120 s^{-1} for MtK379. The rate of the transient phase is the rate of reaching a steady state, which is approximately ($k_3 + k_e$) where k_e is the effective rate of release of products. k_e has to be 20−30 s^{-1} to account for the turnover rate. Thus, k_3 is approximately 100 s^{-1}, which agrees with the value given by Gilbert and Johnson (1994) for the *Drosophila* construct K401.

The rate constant of ADP dissociation (k_5) was not directly measured in the cycle. The rate constant for ADP or mant-ADP dissociation from the MtK·D complex formed by mixing the K·D state with microtubules is 35−40 s^{-1}. In terms of the kinetic scheme, this value also applies to the MtK·D complex formed in the ATPase cycle. It was proposed previously that ADP dissociation is the rate-limiting

step (Hackney, 1988; Gilbert & Johnson, 1994), and the present evidence indicates that the MtK·D state makes up about half the cycle time. However, Gilbert et al. (1995) reported a rate constant of ADP dissociation of 300 s^{-1}. The design of the experiment is identical to the experiments described here, and we have no explanation for the large difference in the results.

The rate constant of phosphate dissociation was not measured. From the values assigned to the rate constants of steps 2, 3, and 5, a maximum steady-state rate of 20−25 s^{-1} requires k_4 to be on the order of 50 s^{-1}. Direct measurements of phosphate dissociation by Gilbert et al. (1995) showed no burst of phosphate release; consequently, the rate of dissociation is not large compared to the steady-state rate. A decrease in fluorescence was obtained with a rate constant of 35−40 s^{-1}. The step in which fluorescence decreases must occur after the hydrolysis step because the rate constant for this step is 100 s^{-1}. Therefore, the decrease may measure the effective rate of the step or steps for the conversion of the high fluorescence MtK·D·P state to the low fluorescence MtK·D and K·D states, although other explanations are possible. The rate constant for the decrease in fluorescence for K379 is 10 s^{-1}, which is equal to the rate constant of the hydrolysis step (k'_3). The assignment of the decrease in fluorescence to a step after hydrolysis is consistent with a rate constant for phosphate dissociation (k'_4) greater than 10 s^{-1}, and the dissociation of phosphate would be rate limited by the hydrolysis step.

It is concluded that binding of K379 to microtubules increases the rate of the hydrolysis step and greatly increases the rate of ADP dissociation, but there may be little effect on the rate of phosphate dissociation.

Reaction Pathway of MtK379 ATPase. At higher ionic strengths or low protein concentrations, the MtK379 complex dissociates during the transient phase. The rate constant of 12 ± 1 s^{-1} for dissociation in 50 mM NaCl is much smaller than the rate of the hydrolysis step of 100 s^{-1}. The results are in agreement with Gilbert et al. (1995), who reported a rate constant for the dissociation of *Drosophila* K401 of 13 s^{-1} at high ionic strength measured by turbidity. If dissociation occurred before hydrolysis, the rate of hydrolysis would be expected to approach the value of 10 s^{-1} for K379, but the observed rate was nearly independent of the degree of dissociation (Figure 9). The results indicate that the main pathway during the transient phase is the formation of MtK·D·P before dissociation. Steady-state binding measurements also gave a smaller dissociation constant of MtK379 in presence of ATP than ADP, which is consistent with the MtK·T and possibly MtK·D·P states in the cycle being more strongly bound than MtK·D.

The ratio of the cycle rate per MtK379 active site to the rate of dissociation of the dimer in 50 mM NaCl is less than 2.5. If this ratio is taken as a measure of processivity, then MtK379 shows low processivity at this ionic strength. Processivity increases at lower ionic strength because the dissociation constant of MtK379 decreases markedly with decreasing ionic strength (Figure 2), but the cycle rate does not (Table 1).

Interactions between Heads of K379. The problem of interaction between heads requires a detailed comparison of the kinetic behavior of monomeric and dimeric kinesin constructs that will be reported elsewhere. The transient and steady-state data for MtK379 are fitted satisfactorily by an independent site model with one exception. The rate constant of substrate binding measured by enhancement of fluorescence did not fit a hyperbolic dependence on concentration, and the intercept of the plot, extrapolated to zero concentration, was less than 1 s^{-1} (Figure 4). The increase in the slope of the plot in the low concentration range is not conclusive evidence for interaction between sites. A similar effect was obtained for the binding of mant-ADP to K379, and it was shown that the effect could be explained quantitatively by an independent site model that takes into account the decrease in fluorescence at a later step (Ma & Taylor, 1995).

However, the three-step model predicts that the rate constant of substrate binding is (k^a[T] + k_e) in the low concentration range; consequently, the intercept is k_e, the effective rate constant of product release. The value is at least 15 s^{-1} for the conditions used for the experiments in 50 mM NaCl. A large limiting value of the rate constant is also obtained by simulation of the complete scheme for a range of values of k^a[T] using KINSIM.

Based on the results of Hackney (1994b), a plausible explanation is that mant-ADP formed by hydrolysis on one head of the MtK379 dimer is released at a rate determined by the binding of mant-ATP to the other head of the dimer. At very low substrate concentrations, this rate is less than 1 s^{-1}.

Comparison of Microtubule Kinesin and Actomyosin Mechanisms. Both mechanisms can be represented by the same form of kinetic scheme. The replacement of MtK in the scheme presented here with AM allows the mechanisms to be compared step by step.

In both cases, the binding of ATP or ADP induces a conformation change that weakens the binding of the motor protein at its actin or microtubule site. The binding constants of K379 and its various nucleotide complexes are strongly dependent on ionic strength, which indicates multiple charge−charge interactions in the binding site, which is also the case for actomyosin.

However, the relative effects of ATP and ADP are reversed in the two mechanisms. The M·T state is weakly bound to actin and dissociates at a rate greater than 1000 s^{-1} while the M·D state is more strongly bound (Ma & Taylor, 1994). In the MtK scheme, K·T appears to be more strongly bound than K·D, and dissociation occurs after the hydrolysis step.

In the actomyosin mechanism, dissociation of phosphate from the M·D·P state is a slow rate-limiting step that is increased 1000-fold by actin binding while phosphate dissociation is relatively fast for K·D·P (> 10 s^{-1}), and the rate may not be changed appreciably by microtubule binding.

The differences in the mechanisms suggest that a different step in the scheme may be coupled to force production and movement. Romberg and Vale (1993) suggested that the force step might occur earlier in the cycle, possibly a transition of an ATP state (step 2 in the scheme). Gilbert et al. (1995) appear to favor an isomerization of the MtK·D·P state. By analogy with the actomyosin mechanism in which a weakly bound state isomerizes to a more strongly bound state, the force step could be assigned to the transition from MtK·D to MtK(D). Further studies are necessary to determine which step is coupled to force generation.

ACKNOWLEDGMENT

We wish to thank Aldona Rukuiza for expert technical assistance.

REFERENCES

Block, S. M., Goldstein, L. S. B., & Schnapp, B. J. (1990) *Nature (London) 348*; 349−352.

Gilbert, S. P., & Johnson, K. A. (1994) *Biochemistry 33*, 1951−1960.

Gilbert, S. P., Webb, M. R., Brune, M., & Johnson, K. A. (1995) *Nature (London) 373*, 671−676.

Hackney, D. D. (1988) *Proc. Natl. Acad. Sci. U.S.A. 85*, 6314−6318.

Hackney, D. D. (1994a) *J. Biol. Chem. 269*, 16508−16511.

Hackney, D. D. (1994b) *Proc. Natl. Acad. Sci. U.S.A. 91*, 6865−6869.

Howard, J., Hudspeth, A. J., & Vale, R. D. (1989) *Nature (London) 342*, 154−158.

Ma, Y. Z., & Taylor, E. W. (1994) *Biophys. J. 66*, 1542−1553.

Ma, Y. Z., & Taylor, E. W. (1995) *Biochemistry 34*, 13233−13241.

Romberg, L., & Vale, R. D. (1993) *Nature (London) 361*, 168−170.

Rosenfeld, S. S., & Taylor, E. W. (1984) *J. Biol. Chem. 259*, 11908−11919.

Sadhu, A., & Taylor, E. W. (1992) *J. Biol. Chem. 267*, 11352−11359.

Svoboda, K., Schmidt, C. F., Schnapp, B. J., & Block, S. M. (1993) *Nature (London) 365*, 721−727.

Trybus, K. M., & Taylor, E. W. (1982) *Biochemistry 21*, 1284−1294.

BI950519L